# Supplementary material

**An open-source population balance modeling framework for the simulation of polydisperse multiphase flows**

Lehnigk R, Bainbridge W, Liao Y, Lucas D, Niemi T, Peltola J, Schlegel F.

AIChE J. 2021

http://doi.org/10.1002/aic.17539

## Solution procedure

The governing equations are solved in a segregated manner using a cell-centered finite volume approach, second order in space and first order in time. The solution sequence for a single outer iteration is summarized in Fig. 1. The pressure-velocity coupling is handled

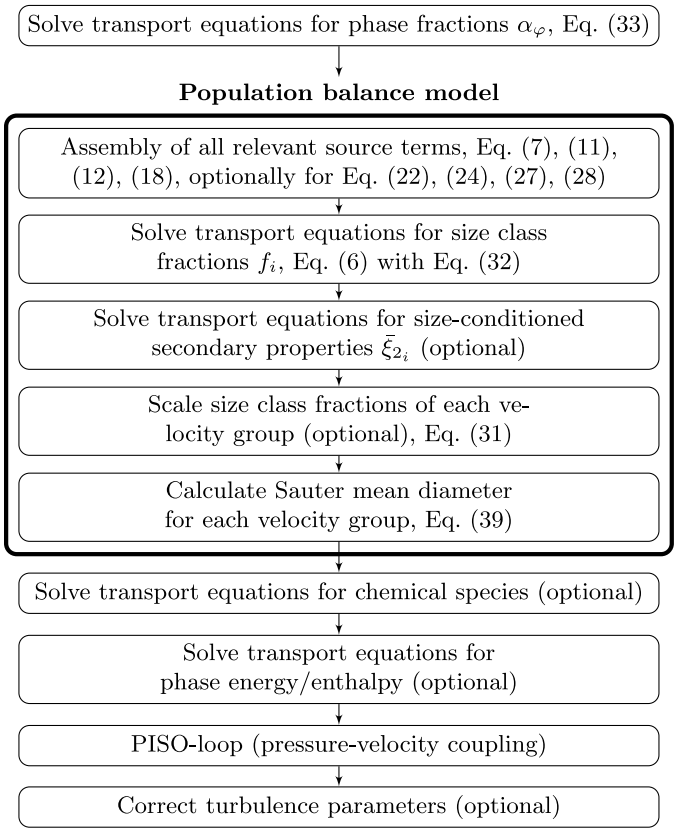


Figure 1: Solution sequence for a single iteration.

using the PISO approach of Issa [1]. The transport equations belonging to the population

balance model are solved after the phase continuity equations but prior to the PISO loop. All relevant source terms within the population balance model are assembled before any transport equation is solved. Since the computation of the coalescence and breakup frequencies is usually the time-consuming part, they are computed once for every relevant size class pair and then used to compute all corresponding source term contributions, i.e. the death terms in the originating classes and the birth term in the resulting class. Furthermore, the implementation exploits the symmetry of the coalescence frequencies and the symmetry of the daughter size distribution function in case of binary breakup.

# Verification

Several tests are performed to verify the implementation of the population balance model. Particular focus is laid on the transfer of secondary particle properties among the size classes. The results are shown in Fig. 2 and 3, wherein the numerical predictions are compared against available analytical or rigorous solutions.

The first case originates from the work of Kumar and Ramkrishna [2] and is used here to test the implementation of their discrete breakup formulation. The underlying scenario is uniform binary breakup according to a power law, given a monodisperse initial condition. An analytical solution is provided by Ziff and McGrady [3]. In the test, the dispersed phase is represented by three velocity groups such that the corresponding continuity equations must be solved alongside the population balance model. The breakup process leads to a mass transfer between those phases. The discrete number density function is reconstructed from the size and velocity group fractions by

$$n_v(x_i) = \frac{f_{i,\varphi}\alpha_\varphi}{x_i(v_{i+1} - v_i)}\,. \tag{1}$$

The numerical and the analytical result agree well as evident from Fig. 2a. Because the mass transfer results in a change of the velocity group fractions, this implies that both the

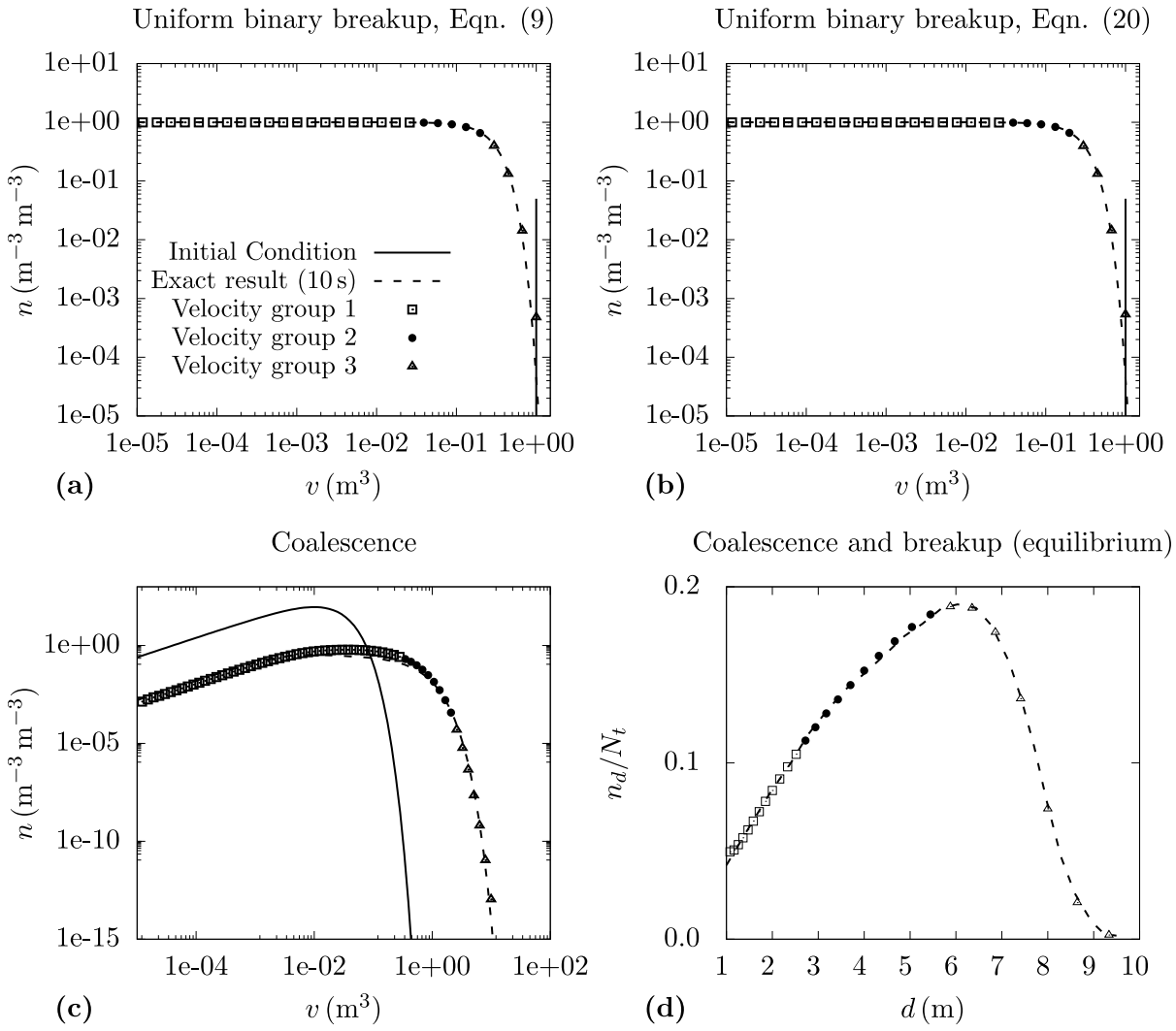


Figure 2: Results of test cases used for verifying the implementation of the coalescence and breakup terms. **(a)** $\tilde{B}_v = v^2 \times 1\,\mathrm{m^{-6}s^{-1}}$, $\beta_{v,v'} = 2/v'$, $x_{i+1}/x_i = 1.5$; **(b)** $\tilde{B}_{v,v'} = 2v' \times 1\,\mathrm{m^{-6}s^{-1}}$, $x_{i+1}/x_i = 1.5$; **(c)** $n_v(t=0) = 25000v\exp(-100v) \times 1\,\mathrm{m^{-9}}$, $\tilde{C}_{v,v'} = 1.0\,\mathrm{m^3s^{-1}}$, $x_{i+1}/x_i = 1.25$; **(d)** $\tilde{C}_{v,v'} = (\sqrt[3]{v} + \sqrt[3]{v'})^3 \times 1\,\mathrm{s^{-1}}$, $\tilde{B}_v = 0.1\exp(0.01v) \times 1\,\mathrm{s^{-1}}$, $\beta_{v,v'} = 2/v'$, $x_{i+1}/x_i = \sqrt[3]{2}$.

implementation of the discrete breakup formulation as well as the accompanied transfer of the secondary property work properly.

The setup of the second case is identical to that of the first, but the alternative discrete formulation for binary breakup of Liao et al. [4] is utilized. Again, the numerical result agrees with the analytical solution (Fig. 2b). Also, the corresponding mass transfer term, i.e. the secondary property treatment, is shown to be implemented correctly.

The third test was also proposed by Kumar and Ramkrishna [2] and is concerned with the implementation of the discrete coalescence terms. An analytical solution is provided by Scott [5]. The distribution is again split into three velocity groups. As shown in Fig. 2c, the numerical solution also agrees well with the analytical solution.

In the fourth case, hydrodynamic coalescence and exponential breakup kernel act simultaneously. Fig. 2d presents the probability density function at equilibrium. A rigorous solution using a large number of sections is available from the work of Vanni [6]. The numerical result also agrees well with the reference solution. This test shows that the basic population balance model and the secondary property transport also work properly in the case that multiple mechanisms are active.

In the main article it was highlighted that the drift term is problematic for all class method approaches using fixed pivots. In the present work, the drift term is applied to predict the isothermal growth of bubbles rising in the direction of decreasing hydrostatic pressure. Although the term does not dominate the solution, i.e. it is not used without coalescence and breakup acting simultaneously, it should be tested whether the applied upwind scheme works for positive (case 5) as well as negative drift (case 6). To this end, a block-shaped number density function is advected along the size coordinate as proposed by Kumar [7]. The discretization for both cases is equidistant in terms of the particle diameter and therefore non-equidistant with a varying section spacing factor with respect to the particle volume. As expected, the number density function diffuses notably (figures 3a and 3c). However, relevant integral properties of the distribution are preserved, as evident from the time evolution of the total particle number concentration

$$N_t = m_0 = \int_0^\infty n_v \mathrm{d}v \approx \sum_{i=0}^{M} N_i \tag{2}$$

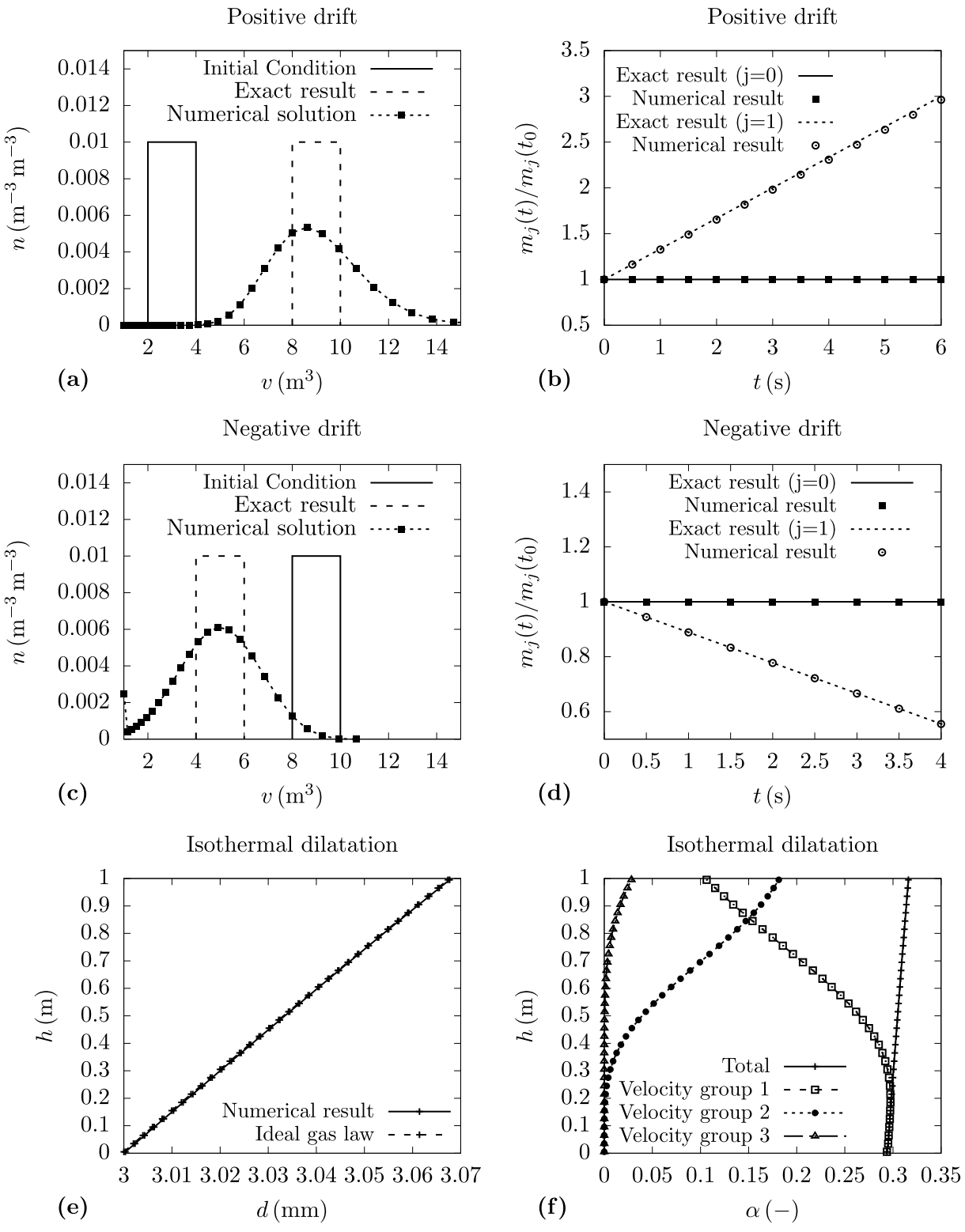


Figure 3: Results of test cases used for verifying the implementation of the drift term. **(a)** & **(b)** $\dot{v}_v = 1\,\mathrm{m}^3\mathrm{s}^{-1}$, $d_{\mathrm{i}+1} = d_{\mathrm{i}} + 0.05\,\mathrm{m}$; **(c)** & **(d)** $\dot{v}_v = -1\,\mathrm{m}^3\mathrm{s}^{-1}$; **(e)** & **(f)** $\dot{v}_v = -v/\rho_d \mathrm{D}\rho_d$, $d_{\mathrm{i}+1} = d_{\mathrm{i}} + 0.01\,\mathrm{mm}$.

and volume concentration

$$\alpha = m_1 = \int_0^\infty v n_v \mathrm{d}v \approx \sum_{i=0}^{M} x_i N_i \tag{3}$$

shown in figures 3b and 3d. The numerical solution matches the exact solution for positive as well as negative drift.

Unfortunately, the setup of cases 5 and 6 does not allow to test the drift-induced mass transfer between the velocity groups. Another test (case 7) is created for this purpose, which simulates the isothermal growth of bubbles rising in a stagnant water column. At the bottom of the one-dimensional domain, the entire dispersed phase fraction is assigned to the first velocity group. As the gas phase rises within the domain, its dilatation translates into a drift of the number density function, causing a continuous mass transfer between the involved velocity groups as shown in Fig. 3f. The drift of the number density function also leads to a change of the diameter. The resulting profile is identical to that obtained from the ideal gas law as shown in Fig. 3e.

In conclusion, the tests show that the implementation is reliable and ready for application to various multiphase flow problems. The population balance model consistently conserves the total mass and number of particles for all relevant mechanisms and is flexible in terms of how the size coordinate is discretized. The source terms describing the transport of the secondary property between the size and velocity groups are also formulated and implemented correctly.

# Computational performance

The computing times reported in Fig. 4 were measured for a single iteration over the entire system of equations (see also Fig. 1). The most dominant part is clearly the population balance model itself, causing up to 75 % of the computional cost. This cost can be split further, showing that particularly the computation of the pairwise coalescence and breakup

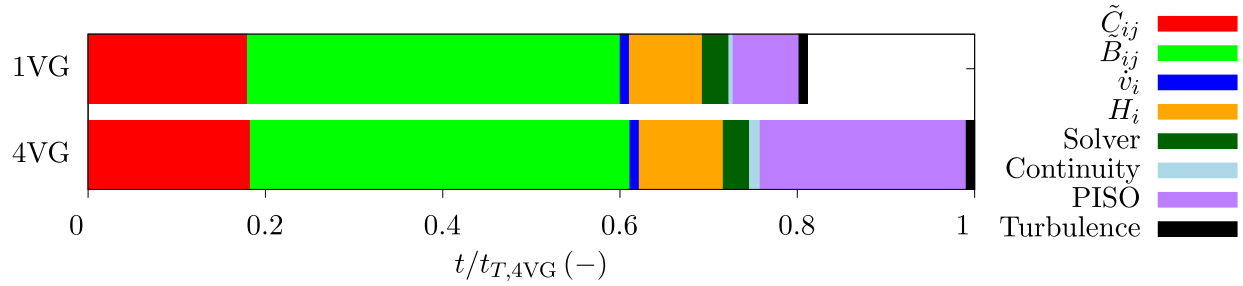


Figure 4: Computational effort associated with calculating coalescence ($\tilde{C}_{ij}$) and binary breakup frequencies ($\tilde{B}_{ij}$) as well as drift rates ($\dot{v}_i$); assembling the source terms for Eq. (6) ($H_i$); assembling the matrices for Eq. (6) and solving the resulting linear equation systems (Solver); solving the continuity equations (Continuity); performing the pressure correction (PISO) and solving the equations belonging to the turbulence model (Turbulence). The reported times are relative to the total computational time required for a simulation using four velocity groups (4VG). For this analysis, all linear solvers where set up to terminate after a single iteration.

frequencies is most expensive, followed directly by the source term assembly using known frequencies. In comparison, the assembly of the matrices for Eq. (6) and the solution of the resulting linear equation systems is cheap in comparison. With four velocity groups, the overall cost for the population balance related source term assembly increases slightly, because the source terms describing the transfer of mass between velocity groups needs to be computed as well. The largest differences between both simulations arise from the solution of the additional continuity and momentum equations. Solving 5 instead of 2 continuity equations takes about 2.5 times longer, i.e. the cost scales linearly. The same change in the number of momentum equations on the other hand leads to an increase of computational time by a factor of 3.1, due to the non-linear increase of the number of involved phase pairs between which interfacial exchanges must be computed.

# References


[1] Issa RI. Solution of the implicitly discretised fluid flow equations by operator-splitting. *Journal of Computational Physics.* 1986;62:40–65.

[2] Kumar S, Ramkrishna D. On the solution of population balance equations by discretization-I. A fixed pivot technique. *Chemical Engineering Science.* 1996;51:1311–1332.

[3] Ziff RM, McGrady ED. The kinetics of cluster fragmentation and depolymerisation. *Journal of Physics A: Mathematical and General.* 1985;18:3027–3037.

[4] Liao Y, Oertel R, Kriebitzsch S, Schlegel F, Lucas D. A discrete population balance equation for binary breakage. *International Journal for Numerical Methods in Fluids.* 2018;87:202–215.

[5] Scott W. Analytical studies in cloud droplet coalescence. *Journal of the Atmospheric Sciences.* 1968;25:54–65.

[6] Vanni M. Approximate Population Balance Equations for Aggregation–Breakage Processes. *Journal of Colloid and Interface Science.* 2000;221:143–160.

[7] Kumar J. *Numerical approximations of population balance equations in particulate systems.* PhD thesisOtto-von-Guericke-Universität Magdeburg 2007.